Electronic Supplementary Material (ESI) for Journal of Materials Chemistry A.
This journal is © The Royal Society of Chemistry 2023

Supporting Information

Mechanistic insights into trisulfur radical generation in lithium−sulfur batteries

Xu Han,[1] Xuefei Xu[1,*]

[1]*Center for Combustion Energy, Department of Energy and Power Engineering, and Key Laboratory for Thermal Science and Power Engineering of Ministry of Education, Tsinghua University, Beijing 100084, China*
*Email: xuxuefei@tsinghua.edu.cn (X. Xu)

Contents

1. Selection and validation of model chemistries

To select appropriate model chemistries, we firstly calculate the reaction energies and forward reaction barriers of the reaction $S_6^{2-} \rightarrow S_3^{\bullet-} + S_3^{\bullet-}$ in gas phase using different model chemistries. The results in Table S1 suggest that MN15/6-311+G(3d2f) and revM06/6-311+G(3d2f) have smaller deviations relative to the benchmark. Because revM06 gives a more precise energy barrier than MN15, and revM06 is thought to perform better in describing intermolecular weak interactions than MN15 based on the tests by Wang *et al*,[1] we conclude that revM06 is the most suitable functional for our system.

However, given that geometric optimizations using revM06/6-311+G(3d2f) is expensive when too many explicit solvent molecules are considered, we make the following comparsions in Table S2 and Table S3 using two different combinations of model chemistries, namely revM06/$BASE^L$//revM06/$BASE^S$ (denoted as Model1) and revM06/$BASE^L$ (denoted as Model2). The maximum unsigned deviation of reaction energies, forward reaction barriers, and binding energies using Model1 relative to corresponding values by Model2 are only 0.05, 0.05, and 0.07 kcal/mol, respectively. It suggests our calculations based on Model1 are accurate enough.

Therefore, we employ revM06/$BASE^L$//revM06/$BASE^S$ model chemistry to calculate the energetis in this work.

Table S1. Reaction energies (ΔE, in kcal/mol) and forward reaction barriers ($\Delta E^{\ddagger}$, in kcal/mol) of the reaction $S_6^{2-} \rightarrow S_3^{\bullet-} + S_3^{\bullet-}$ in gas phase calculated by various model chemistries and the corresponding deviations from the benchmark.

method[a]	ΔE	UD(ΔE)	$\Delta E^{\ddagger}$	UD($\Delta E^{\ddagger}$)	MUD[b]
MN15	−45.21	0.08	12.62	1.45	0.77
revM06	−46.36	1.23	11.84	0.67	0.95
M06	−45.40	0.27	9.51	1.66	0.97
M06-2X	−45.49	0.36	13.06	1.88	1.12
M05-2X	−47.88	2.75	11.35	0.18	1.47
M08-HX	−46.15	1.02	13.46	2.29	1.65
M08-SO	−44.53	0.60	13.99	2.81	1.71
ωB97X-D	−47.89	2.76	12.58	1.41	2.08
PWB6K	−49.08	3.95	11.56	0.39	2.17
N12-SX	−47.93	2.80	9.07	2.10	2.45
APFD	−47.62	2.49	8.64	2.53	2.51
M11	−47.84	2.71	13.78	2.60	2.66
BMK	−43.03	2.10	15.07	3.90	3.00
MN12-SX	−48.84	3.71	8.22	2.96	3.34
PW6B95-D3	−48.94	3.81	8.15	3.02	3.42
PBE0	−49.43	4.30	8.18	2.99	3.65
revM11	−43.72	1.42	17.07	5.90	3.66
B97-1	−48.57	3.44	7.20	3.98	3.71

B97-3	−50.08	4.95	8.39	2.79	3.87
MN15-L	−48.05	2.92	5.98	5.20	4.06
HSE06	−49.70	4.57	7.17	4.00	4.28
revM06-L	−48.62	3.49	6.10	5.08	4.29
M06-HF	−42.22	2.91	16.96	5.78	4.35
PBEsol	−45.12	0.01	2.44	8.74	4.38
MN12-L	−47.94	2.81	5.23	5.94	4.38
B3LYP	−48.91	3.78	6.11	5.06	4.42
PW6B95	−51.00	5.87	7.50	3.67	4.77
GVWN3	−38.98	6.15	3.91	7.27	6.71
N12	−50.79	5.66	1.93	9.24	7.45
TPSSh	−52.46	7.33	3.41	7.77	7.55
PBE	−49.70	4.56	0.53	10.65	7.61
M06-L	−50.80	5.67	1.06	10.11	7.89
TPSS	−52.74	7.61	−0.12	11.30	9.45
GAM	−53.32	8.18	−0.16	11.33	9.76
revPBE	−53.88	8.75	−0.75	11.93	10.34
M11-L	−56.13	11.00	−1.42	12.60	11.80
OreLYP	−57.49	12.36	−1.23	12.40	12.38
HLE17	−60.85	15.72	0.21	10.96	13.34
WMS	**−45.13**	**0.00**	**11.17**	**0.00**	**0.00**

[a]The energies are based on the geometries optimized by M06-2X/6-311+G(3d2f). All density functionals use the 6-311+G(3d2f) basis set, and WMS is the benchmark method.

[b]UD and MUD are unsigned deviation and mean unsigned deviation from the benchmark, respectively.

Table S2. Comparison of reaction energies (ΔE, in kcal/mol) and forward reaction barriers ($\Delta E^{\ddagger}$, in kcal/mol) of some S−S bond cleavage reactions in solution calculated by two different model chemistries (Model1 and Model2).

implicit solvent	S−S bond cleavage reaction	ΔE			$\Delta E^{\ddagger}$		
		Model1	Model2	UD	Model1	Model2	UD
DMSO	$Li_2S_6 \rightarrow LiS_3^{\bullet}–LiS_3^{\bullet}$	6.85	6.84	0.01	17.43	17.45	0.02
	$LiS_6^{-} \rightarrow LiS_3^{\bullet}–S_3^{\bullet-}$	7.08	7.08	0.00	13.87	13.88	0.01
	$S_6^{2-} \rightarrow S_3^{\bullet-}–S_3^{\bullet-}$	7.42	7.45	0.03	8.53	8.58	0.05
DOL	$Li_2S_6 \rightarrow LiS_3^{\bullet}–LiS_3^{\bullet}$	6.92	6.92	0.00	17.23	17.25	0.02
	$LiS_6^{-} \rightarrow LiS_3^{\bullet}–S_3^{\bullet-}$	6.20	6.20	0.00	13.06	13.05	0.01
	$S_6^{2-} \rightarrow S_3^{\bullet-}–S_3^{\bullet-}$	8.28	8.33	0.05	9.25	9.30	0.05

Table S3. Comparison of binding energies (E_b, in kcal/mol) calculated by two different model chemistries (Model1 and Model2).

implicit solvent	system	E_b		
		Model1	Model2	UD
DMSO	Li_2S_6 + DMSO	−17.37	−17.30	0.07
	LiS_6^- + DMSO	−16.71	−16.70	0.01
	S_6^{2-} + DMSO	−4.41	−4.39	0.02
	$LiS_3^\bullet$ + DMSO	−20.17	−20.14	0.03
	$S_3^{\bullet-}$ + DMSO	−3.40	−3.38	0.02
DOL	Li_2S_6 + DOL	−14.55	−14.52	0.03
	LiS_6^- + DOL	−12.97	−12.94	0.03
	S_6^{2-} + DOL	−5.06	−5.04	0.02
	$LiS_3^\bullet$ + DOL	−15.02	−15.02	0.00
	$S_3^{\bullet-}$ + DOL	−3.45	−3.46	0.01

Table S4. Interaction energies (δE, in kcal/mol) between two fragments inside a molecule and corresponding basis set superposition error (BSSE, in kcal/mol).

molecule[a]	fragment 1	fragment 2	δE[b]	BSSE	$\frac{\delta E}{\text{BSSE}}$
$Li^+(DMSO)_4$	$Li^+(DMSO)_3$	DMSO	−34.43	1.54	4.48%
$Li^+(DMSO)_5$	$Li^+(DMSO)_4$	DMSO	−26.24	1.65	6.30%
$Li^+(DMSO)_6$	$Li^+(DMSO)_5$	DMSO	−27.44	2.03	7.41%
$Li^+(DOL)_4$	$Li^+(DOL)_3$	DOL	−26.55	1.47	5.55%
$Li^+(DOL)_5$	$Li^+(DOL)_4$	DOL	−20.47	1.69	8.26%
$Li^+(DOL)_6$	$Li^+(DOL)_5$	DOL	−23.08	1.93	8.35%

[a]The molecule consists of fragment 1 and fragment 2.

[b]δE are calculated by the difference of potential energies between the molecule and the fragments in gas phase because corresponding BSSE corrections are also estimated at the same level.

2. Calculation setups for simulating different solvent systems based on the SMD solvation model

Table S5. Calculation setups in Gaussian 09 program for different solvent systems.

solvent	keywords	parameters[a]
DMSO	*scrf=(smd,solvent=dmso)*	
DOL	*scrf(read,SMD,solvent=generic)*	*eps=7.34* *epsinf=1.396* *HBondAcidity=0.00* *HBondBasicity=0.64* *SurfaceTensionAtInterface=46.85* *CarbonAromaticity=0.00* *ElectronegativeHalogenicity=0.00*
DMA	*scrf(read,SMD,solvent=generic)*	*eps=37.781* *epsinf=2.062* *HBondAcidity=0.00* *HBondBasicity=0.7* *SurfaceTensionAtInterface=47.62* *CarbonAromaticity=0.00* *ElectronegativeHalogenicity=0.00*

[a]No external SMD calculation parameters are used for DMSO, because DMSO is incorporated in the internal solvent database of Gaussian 09.

3. Structures and stability of sulfur species and Li^+ in solution

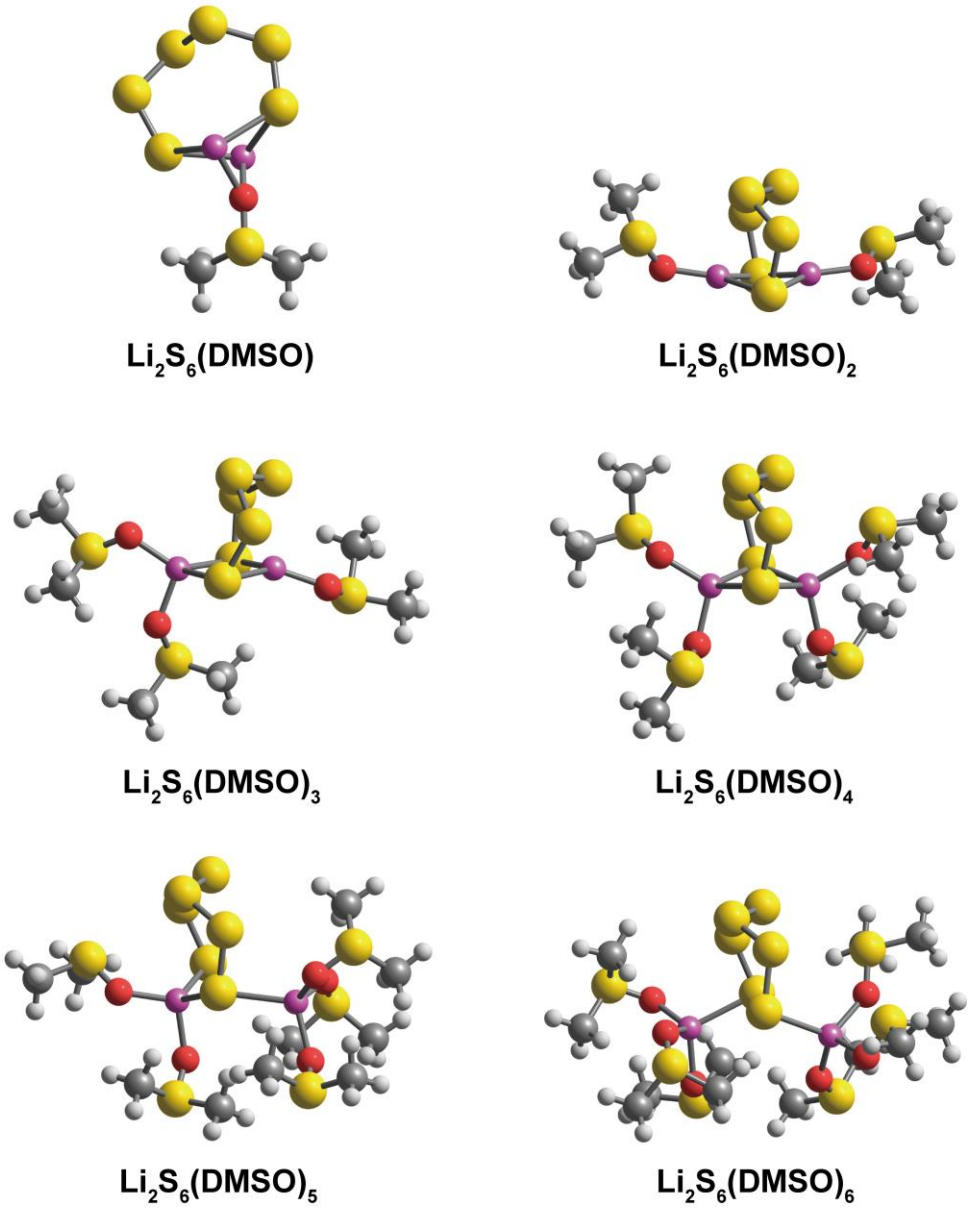

Fig. S1. Optimized solvation structures of Li_2S_6 in DMSO. Color scheme: H, light gray; Li, purple; C, gray; O, red; S, yellow.

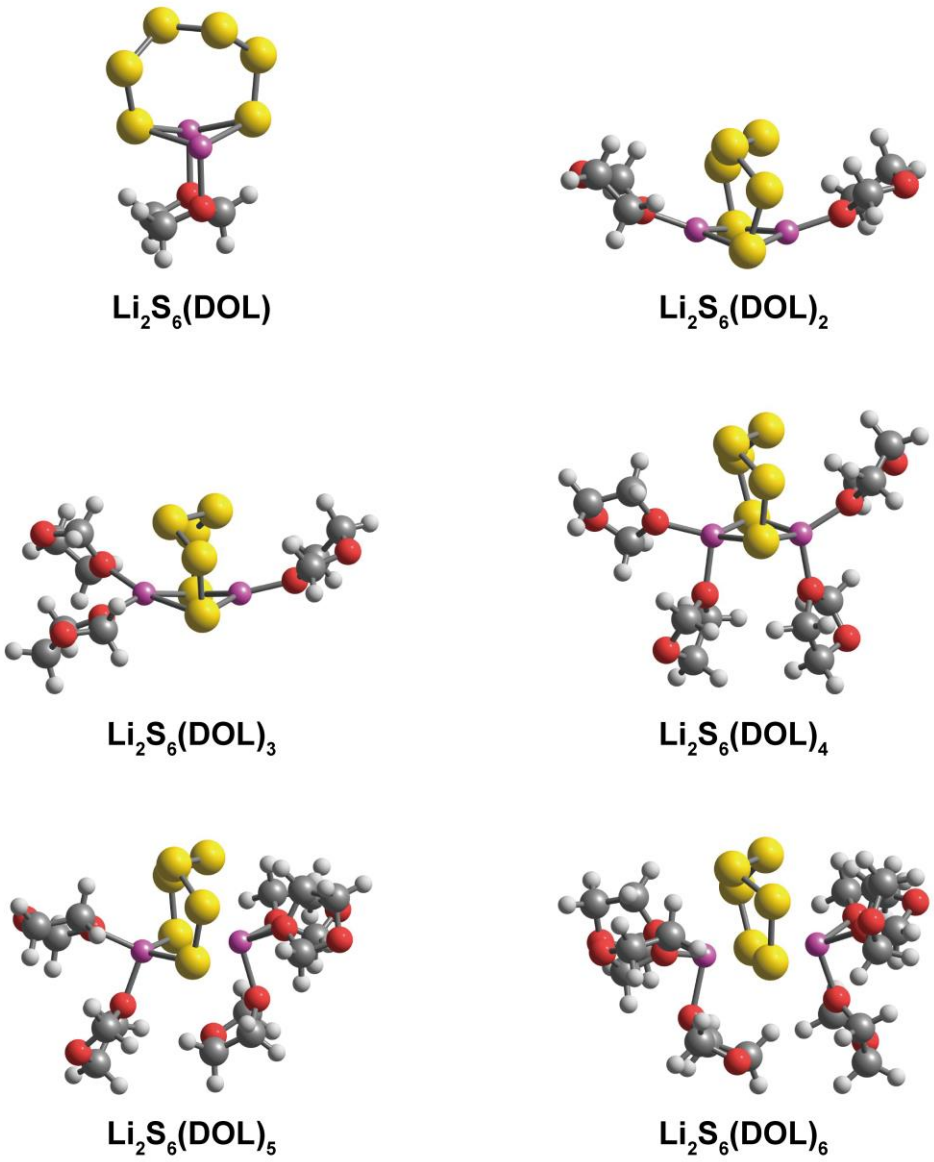

Fig. S2. Optimized solvation structures of Li_2S_6 in DOL.

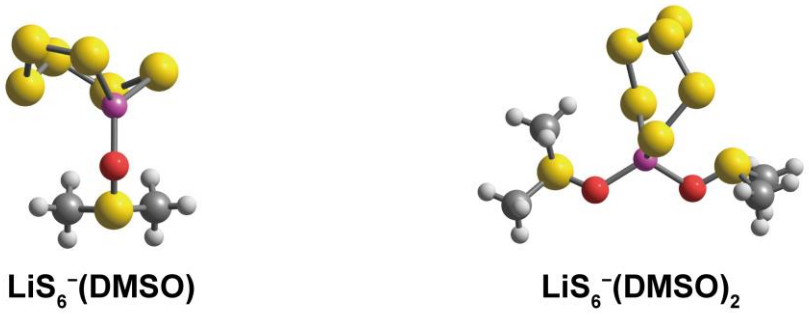

Fig. S3. Optimized solvation structures of LiS_6^- in DMSO.

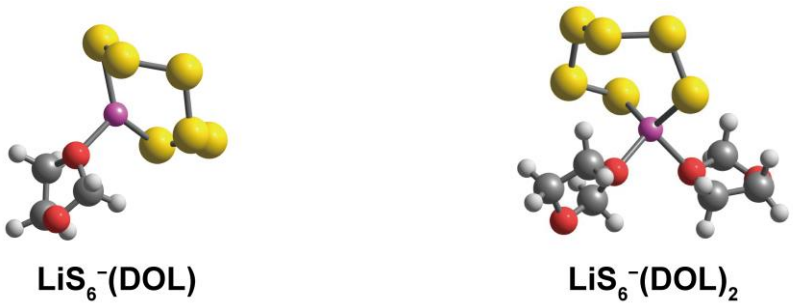

Fig. S4. Optimized solvation structures of LiS_6^- in DOL.

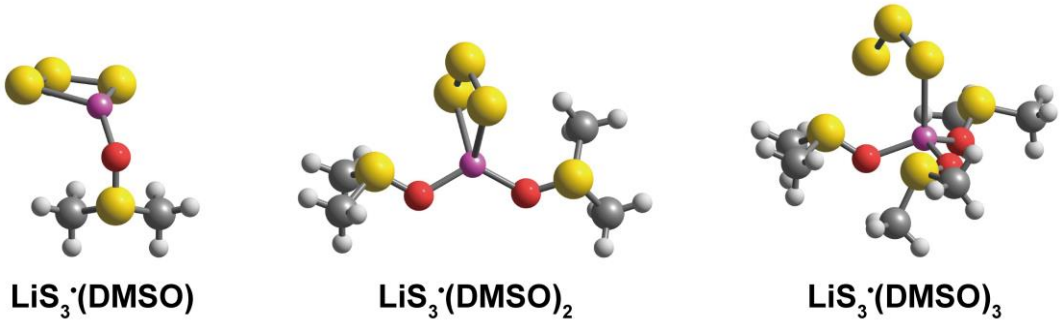

Fig. S5. Optimized solvation structures of $LiS_3^{\bullet}$ in DMSO.

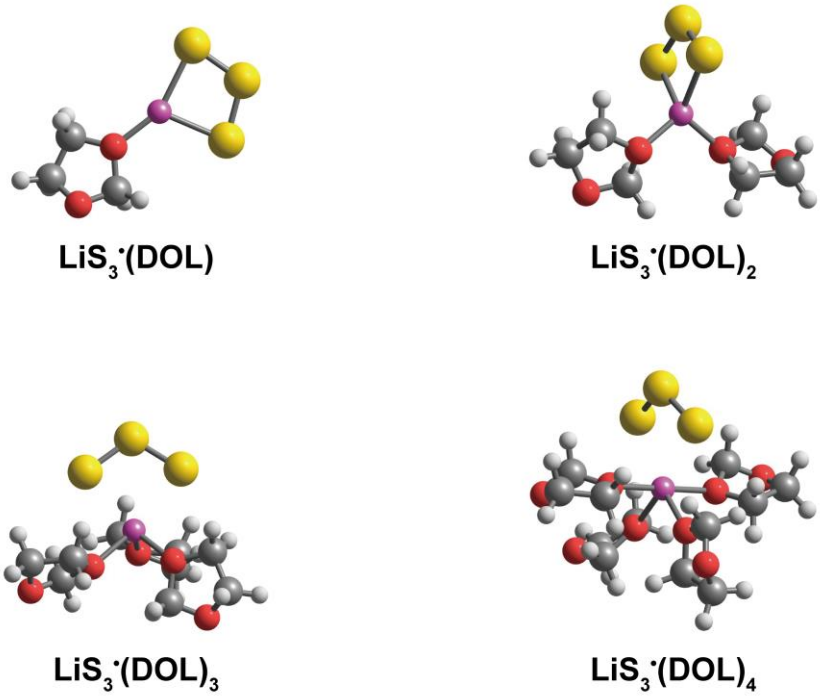

Fig. S6. Optimized solvation structures of $LiS_3^{\bullet}$ in DOL.

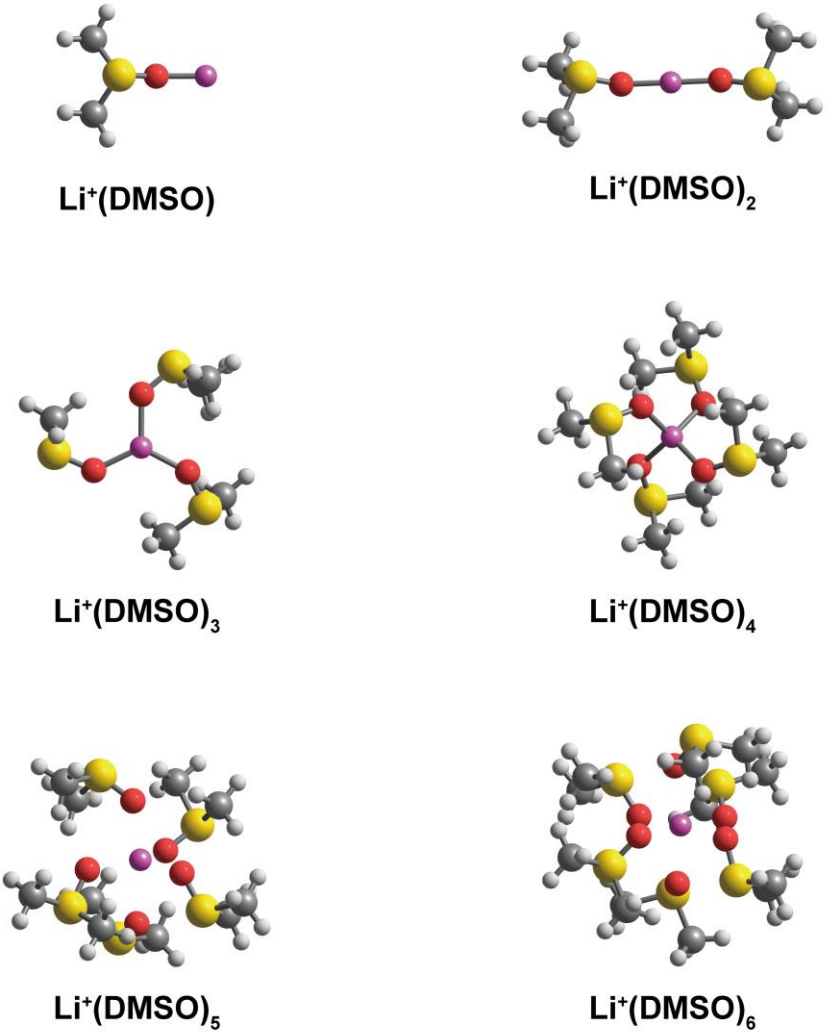

Fig. S7. Optimized solvation structures of Li^+ in DMSO.

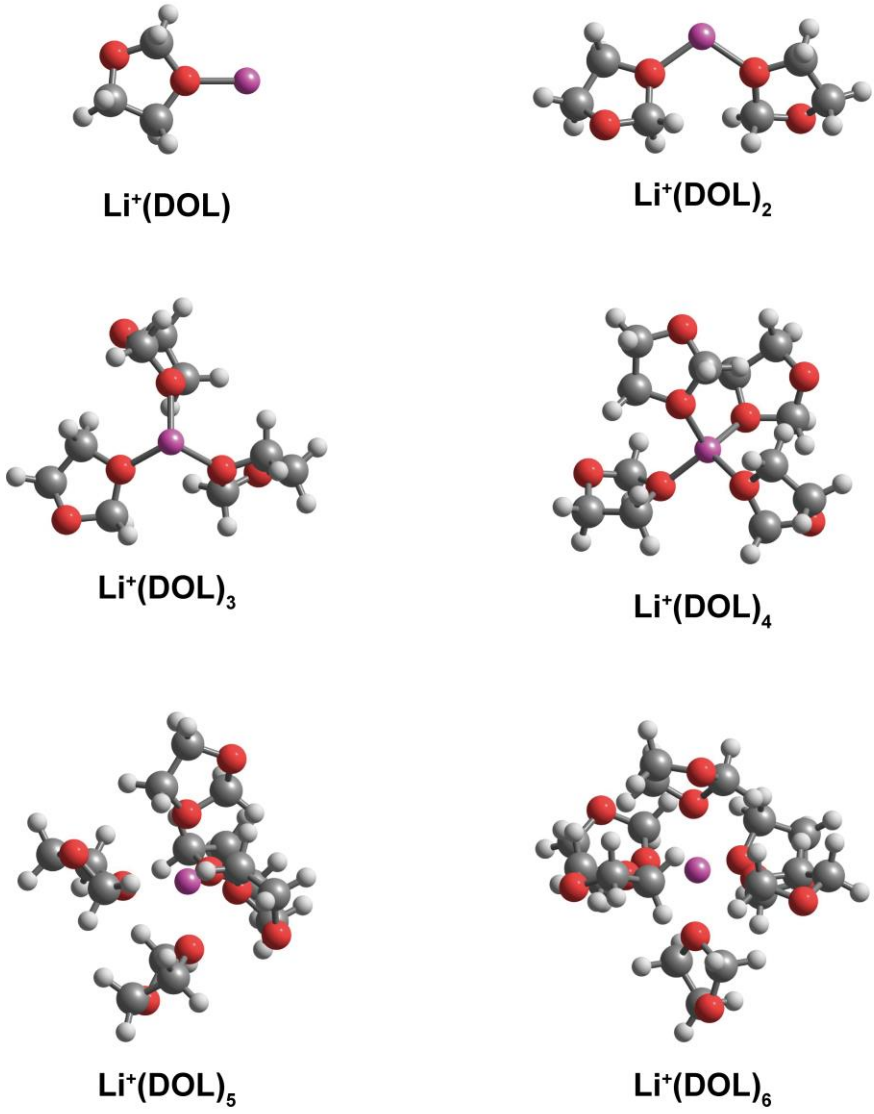

Fig. S8. Optimized solvation structures of Li^+ in DOL.

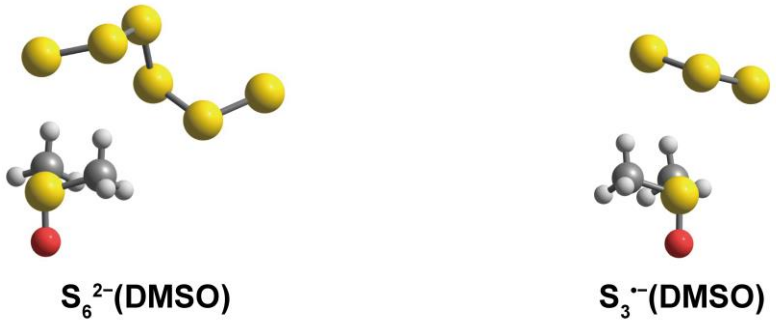

Fig. S9. Optimized solvation structures of S_6^{2-} and $S_3^{\bullet-}$ in DMSO.

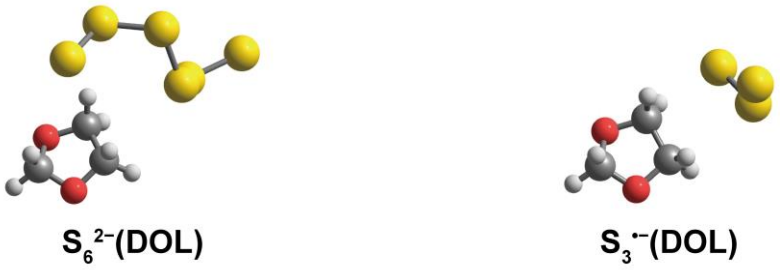

Fig. S10. Optimized solvation structures of S_6^{2-} and $S_3^{\bullet-}$ in DOL.

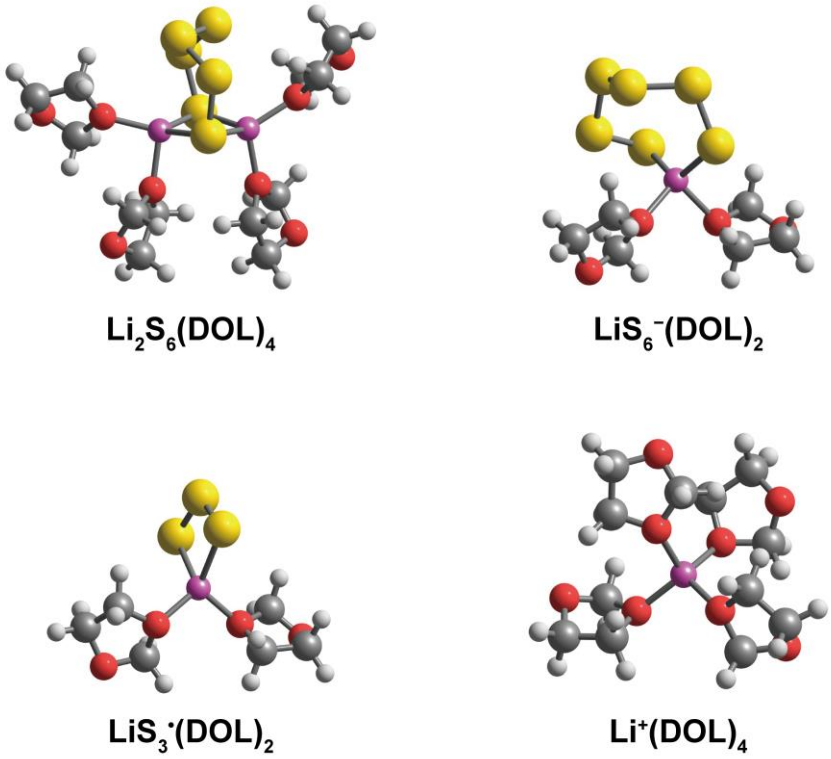

Fig. S11. Optimized solvation structures of Li_2S_6, LiS_6^-, $LiS_3^\bullet$, and Li^+ with the best NCS in DOL.

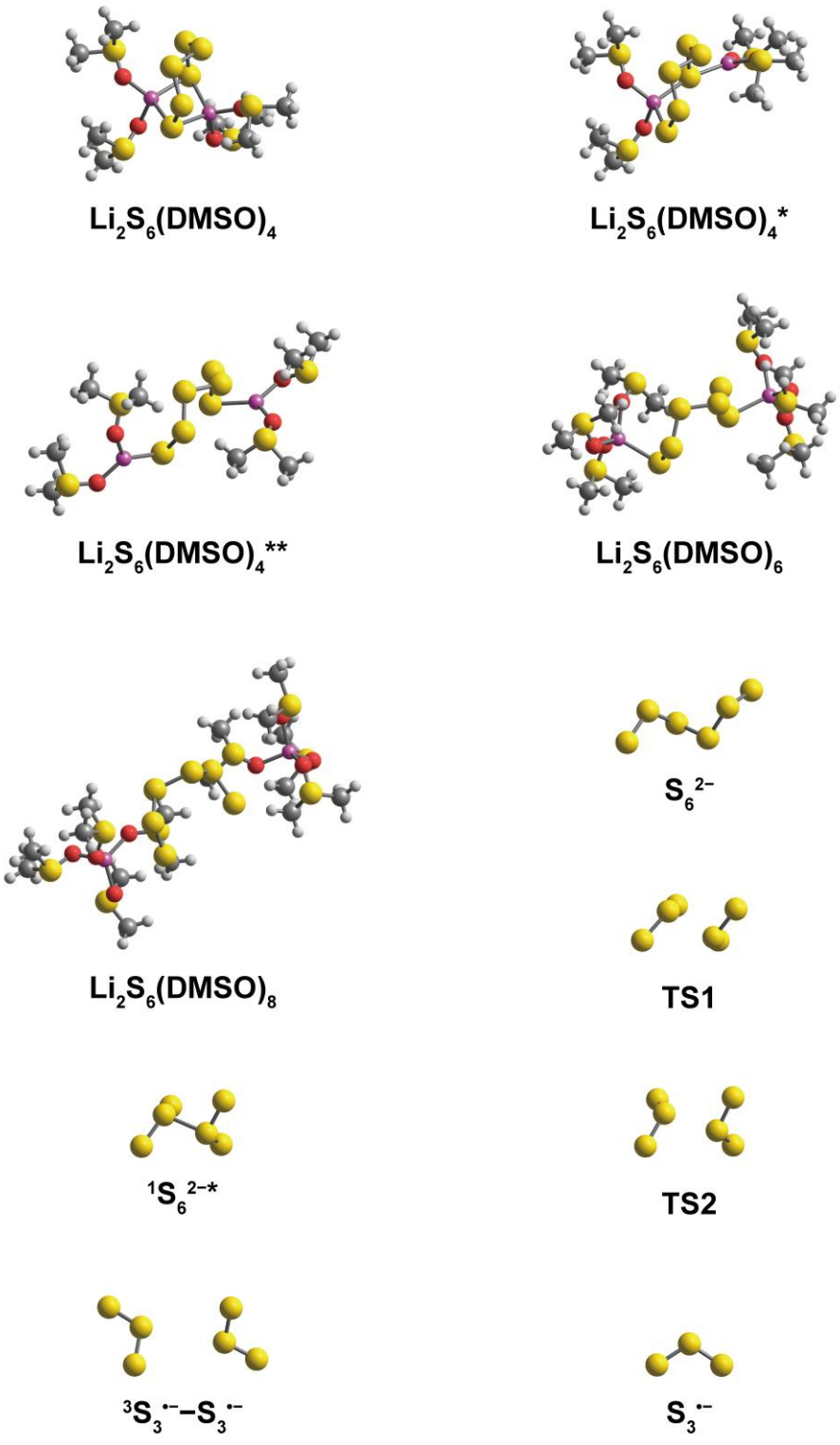

Fig. S12. Optimized intermediate or transition state solvation structures in the reaction of $Li_2S_6(DMSO)_4$ + 4DMSO → $2S_3^{\bullet-}$ + $2Li^+(DMSO)_4$.

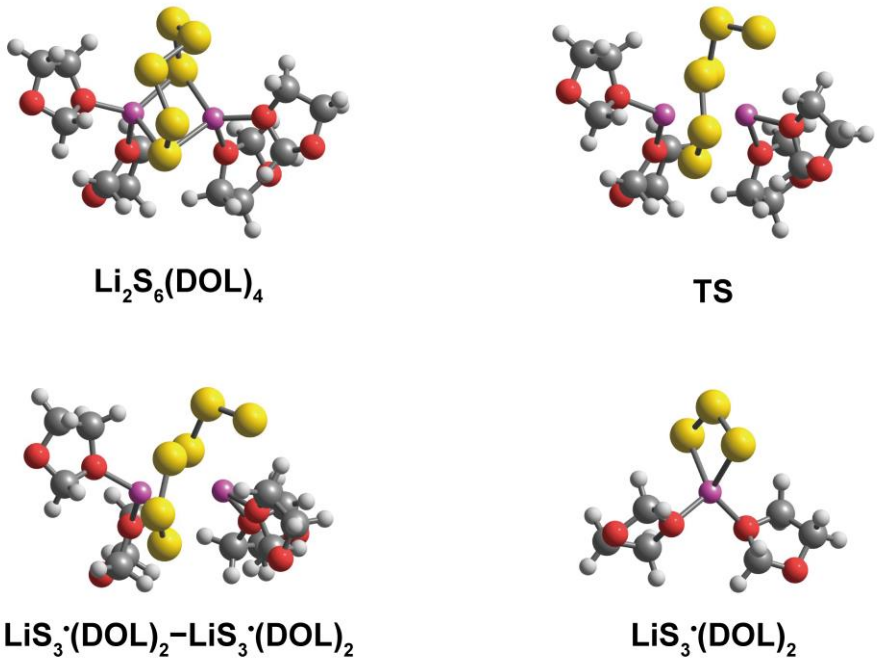

Fig. S13. Optimized intermediate or transition state solvation structures in the reaction of $Li_2S_6(DOL)_4 \rightarrow 2LiS_3^{\bullet}(DOL)_2$.

Table S6. Energy components of interactions (in kcal/mol) between two fragments inside a molecule.

molecule[a]	fragment 1	fragment 2	interactions between two fragments[b]			
			electrostatics	exchange	induction	dispersion
$Li^+(DMSO)_4$	$Li^+(DMSO)_3$	DMSO	−34.86	28.18	−12.01	−13.18
$Li^+(DMSO)_5$	$Li^+(DMSO)_4$	DMSO	−27.45	26.48	−8.80	−14.25
$Li^+(DOL)_4$	$Li^+(DOL)_3$	DOL	−23.68	19.19	−9.27	−10.37
$Li^+(DOL)_5$	$Li^+(DOL)_4$	DOL	−20.92	24.68	−6.38	−15.13

[a]The molecule consists of fragment 1 and fragment 2.

[b]This energy decomposition analysis based on symmetry-adapted perturbation theory (SAPT)[2] is performed by PSI4 1.4 software[3] with SAPT2+/aug-cc-pVDZ method in gas phase to understand the non-covalent interactions. The interaction energy between two fragments can be divided into four parts: electrostatics, exchange, induction, and dispersion.

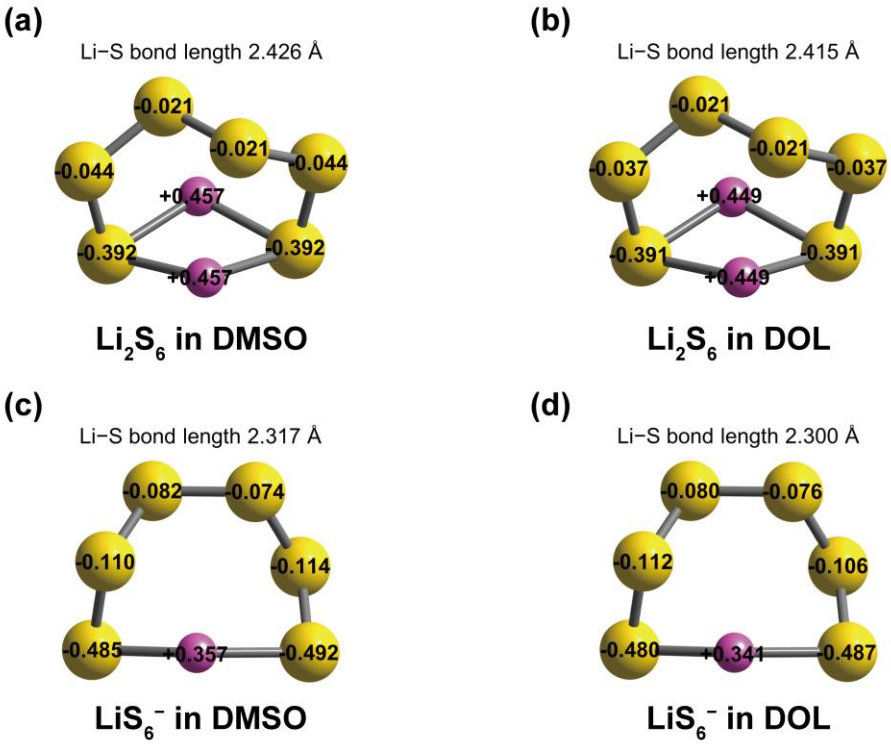

Fig. S14. Charge distribution and average Li−S bond lengths of (a) Li_2S_6 in DMSO; (b) Li_2S_6 in DOL; (c) LiS_6^- in DMSO; (d) LiS_6^- in DOL. Here no explicit solvent molecules but implicit polarity environment are considered. The atomic charges are quantified based on the CM5 charge model.[4]

Table S7. Bond dissociation energies (ΔE, in kcal/mol) of Li−S and S−S bond.

bond	ΔE^a	
	in DMSO	in DOL
Li−S	98.28	94.78
S−S	107.53	107.67

[a]Dissociation energy of A−B bond is estimated by the reaction energy of homolytic bond cleavage reaction (A + B → A−B).

4. Energetics of revelant reactions in the generation of radicals in solution

Table S8. Reaction free energies (ΔG_r, in kcal/mol) of R1 when considering the solvation structures with all possible NCS.

coefficient in R1[a]				ΔG_r[b]		coefficient in R1				ΔG_r	
m	n	p	q	DMSO	DOL	m	n	p	q	DMSO	DOL
2	0	1	1	**15.17**	**30.42**	5	0	1	4	**−3.47**	13.49
3	0	1	2	**7.84**	**23.00**	5	0	2	3	1.38	16.70
3	0	2	1	17.50	28.24	5	1	1	5	8.25	15.43
4	0	1	3	2.30	20.78	5	1	2	4	**−3.47**	**12.48**
4	0	2	2	8.23	25.67	5	2	1	6	15.47	26.44
4	1	1	4	**−2.55**	16.57	5	2	2	5	8.25	14.41
4	1	2	3	2.31	19.77	5	3	2	6	15.48	25.43
4	2	1	5	9.17	18.50	6	0	1	5	−1.93	10.41
4	2	2	4	**−2.54**	**15.55**	6	0	2	4	**−13.64**	**7.46**
4	3	1	6	16.40	29.52	6	1	1	6	5.30	21.42
4	3	2	5	9.18	17.49	6	1	2	5	−1.92	9.39
4	4	2	6	16.41	28.50	6	2	2	6	5.31	20.41

[a]R1: $Li_2S_6(sol)_m + nsol \rightarrow LiS_6^-(sol)_p + Li^+(sol)_q$.

[b]The lowest ΔG_r are in bold for each NCS in reactants.

Table S9. Reaction free energies (ΔG_r, in kcal/mol) of R2 when considering the solvation structures with all possible NCS.

coefficient in R2[a]				ΔG_r[b]		coefficient in R2				ΔG_r	
m	n	p	q	DMSO	DOL	m	n	p	q	DMSO	DOL
2	0	1	1	**36.49**	**76.29**	5	2	2	5	19.92	55.05
3	0	1	2	**29.16**	**68.87**	5	2	3	4	2.28	47.21
3	0	2	1	**29.16**	**68.87**	5	2	4	3	2.28	47.21
4	0	1	3	23.63	66.66	5	2	5	2	19.92	55.05
4	0	2	2	19.89	66.30	5	2	6	1	36.80	72.32
4	0	3	1	23.63	66.66	5	3	2	6	27.15	66.06
4	1	1	4	18.78	62.44	5	3	3	5	14.00	49.15
4	1	2	3	13.97	60.40	5	3	4	4	**−2.57**	**43.00**
4	1	3	2	13.97	60.40	5	3	5	3	14.00	49.15
4	1	4	1	18.78	62.44	5	3	6	2	27.15	66.06
4	2	1	5	30.50	64.37	5	4	3	6	21.23	60.16
4	2	2	4	9.12	56.19	5	4	4	5	9.15	44.93
4	2	3	3	8.06	54.50	5	4	5	4	9.15	44.93
4	2	4	2	9.12	56.19	5	4	6	3	21.23	60.16
4	2	5	1	30.50	64.37	5	5	4	6	16.38	55.95
4	3	1	6	37.72	75.39	5	5	5	5	20.87	46.86
4	3	2	5	20.84	58.12	5	5	6	4	16.38	55.95
4	3	3	4	3.21	50.29	5	6	5	6	28.10	57.88
4	3	4	3	3.21	50.29	5	6	6	5	28.10	57.88
4	3	5	2	20.84	58.12	5	7	6	6	35.33	68.89
4	3	6	1	37.72	75.39	6	0	1	5	19.40	56.28
4	4	2	6	28.07	69.14	6	0	2	4	−1.97	48.09
4	4	3	5	14.93	52.22	6	0	3	3	−3.04	46.41
4	4	4	4	**−1.64**	**46.07**	6	0	4	2	−1.97	48.09
4	4	5	3	14.93	52.22	6	0	5	1	19.40	56.28
4	4	6	2	28.07	69.14	6	1	1	6	26.63	67.29
4	5	3	6	22.16	63.24	6	1	2	5	9.75	50.03
4	5	4	5	10.08	48.00	6	1	3	4	−7.89	42.19
4	5	5	4	10.08	48.00	6	1	4	3	−7.89	42.19
4	5	6	3	22.16	63.24	6	1	5	2	9.75	50.03
4	6	4	6	17.30	59.02	6	1	6	1	26.63	67.29
4	6	5	5	21.80	49.94	6	2	2	6	16.97	61.04
4	6	6	4	17.30	59.02	6	2	3	5	3.83	44.13
4	7	5	6	29.02	60.95	6	2	4	4	**−12.74**	**37.97**
4	7	6	5	29.02	60.95	6	2	5	3	3.83	44.13
4	8	6	6	36.25	71.97	6	2	6	2	16.97	61.04
5	0	1	4	17.85	59.37	6	3	3	6	11.06	55.14
5	0	2	3	13.05	57.33	6	3	4	5	−1.02	39.91

5	0	3	2	13.05	57.33	6	3	5	4	−1.02	39.91
5	0	4	1	17.85	59.37	6	3	6	3	11.06	55.14
5	1	1	5	29.57	61.30	6	4	4	6	6.21	50.92
5	1	2	4	8.20	53.11	6	4	5	5	10.70	41.84
5	1	3	3	7.13	51.43	6	4	6	4	6.21	50.92
5	1	4	2	8.20	53.11	6	5	5	6	17.93	52.86
5	1	5	1	29.57	61.30	6	5	6	5	17.93	52.86
5	2	1	6	36.80	72.32	6	6	6	6	25.15	63.87

[a]R2: $Li_2S_6(sol)_m + nsol \rightarrow S_6^{2-} + Li^+(sol)_p + Li^+(sol)_q$.

[b]The lowest ΔG_r are in bold for each NCS in reactants.

Table S10. Reaction free energies (ΔG_r, in kcal/mol) of R3 when considering the solvation structures with all possible NCS.

coefficient in R3[a]			ΔG_r[b]	
m	n	p	DMSO	DOL
1	0	1	**21.33**	**45.87**
2	0	2	11.66	40.64
2	1	3	5.75	34.73
2	2	4	**0.90**	**30.52**
2	3	5	12.62	32.45
2	4	6	19.85	43.47

[a]R3: $LiS_6^-(sol)_m + nsol \rightarrow S_6^{2-} + Li^+(sol)_p$.

[b]The lowest ΔG_r are in bold for each NCS in reactants.

Table S11. Reaction free energies (ΔG_r, in kcal/mol) of R4 when considering the solvation structures with all possible NCS.

coefficient in R4[a]				ΔG_r[b]		coefficient in R4				ΔG_r	
m	n	p	q	DMSO	DOL	m	n	p	q	DMSO	DOL
2	0	1	1	**14.95**	**18.85**	5	0	2	3	7.21	10.05
3	0	1	2	**11.86**	**12.90**	5	0	3	2	7.21	10.05
3	0	2	1	11.86	12.90	5	0	4	1	N/A	18.38
4	0	1	3	13.55	17.91	5	1	2	4	N/A	13.59
4	0	2	2	**6.82**	**11.80**	5	1	3	3	8.52	11.38
4	0	3	1	13.55	17.91	5	1	4	2	N/A	13.59
4	1	1	4	N/A	21.45	5	2	3	4	N/A	14.91
4	1	2	3	8.13	13.12	5	2	4	3	N/A	14.91
4	1	3	2	8.13	13.12	5	3	4	4	N/A	18.45
4	1	4	1	N/A	21.45	6	−2	2	2	**−4.27**	**3.70**
4	2	2	4	N/A	16.66	6	−1	2	3	−2.96	5.03
4	2	3	3	9.44	14.45	6	−1	3	2	−2.96	5.03
4	2	4	2	N/A	16.66	6	0	2	4	N/A	8.57
4	3	3	4	N/A	17.99	6	0	3	3	−1.66	6.35
4	3	4	3	N/A	17.99	6	0	4	2	N/A	8.57
4	4	4	4	N/A	21.53	6	1	3	4	N/A	9.89
5	−1	2	2	**5.90**	**8.73**	6	1	4	3	N/A	9.89
5	0	1	4	N/A	18.38	6	2	4	4	N/A	13.43

[a]R4: $Li_2S_6(sol)_m + nsol \rightarrow LiS_3^{\bullet}(sol)_p + LiS_3^{\bullet}(sol)_q$.

[b]The lowest ΔG_r are in bold for each NCS in reactants.

Table S12. Reaction free energies (ΔG_r, in kcal/mol) of R5 when considering the solvation structures with all possible NCS.

coefficient in R5[a]				ΔG_r[b]		coefficient in R5				ΔG_r	
m	n	p	q	DMSO	DOL	m	n	p	q	DMSO	DOL
2	0	1	1	**25.48**	**43.75**	5	1	5	1	18.56	28.76
3	0	2	1	**18.15**	**36.33**	5	1	4	2	**1.42**	**22.04**
3	0	1	2	22.38	37.80	5	1	3	3	7.58	27.58
4	0	3	1	12.61	34.11	5	1	2	4	N/A	37.02
4	0	2	2	13.11	35.23	5	2	6	1	25.78	39.77
4	0	1	3	24.08	42.80	5	2	5	2	13.14	23.97
4	1	4	1	7.76	29.90	5	2	4	3	2.73	23.36
4	1	3	2	7.20	29.33	5	2	3	4	N/A	31.12
4	1	2	3	14.42	36.55	5	3	6	2	20.37	34.98
4	1	1	4	N/A	46.34	5	3	5	3	14.45	25.29
4	2	5	1	19.48	31.83	5	3	4	4	N/A	26.90
4	2	4	2	**2.35**	**25.11**	5	4	6	3	21.68	36.31
4	2	3	3	8.51	30.65	5	4	5	4	N/A	28.83
4	2	2	4	N/A	40.09	5	5	6	4	N/A	39.85
4	3	6	1	26.71	42.85	6	0	5	1	8.38	23.74
4	3	5	2	14.07	27.04	6	0	4	2	**−8.75**	**17.01**
4	3	4	3	3.65	26.43	6	0	3	3	−2.59	22.56
4	3	3	4	N/A	34.19	6	0	2	4	N/A	32.00
4	4	6	2	21.29	38.06	6	1	6	1	15.61	34.75
4	4	5	3	15.37	28.37	6	1	5	2	2.97	18.95
4	4	4	4	N/A	29.97	6	1	4	3	−7.44	18.34
4	5	6	3	22.60	39.38	6	1	3	4	N/A	26.10
4	5	5	4	N/A	31.91	6	2	6	2	10.20	29.96
4	6	6	4	N/A	42.92	6	2	5	3	4.28	20.27
5	0	4	1	6.84	26.82	6	2	4	4	N/A	21.88
5	0	3	2	6.27	26.25	6	3	6	3	11.50	31.29
5	0	2	3	13.50	33.48	6	3	5	4	N/A	23.81
5	0	1	4	N/A	43.27	6	4	6	4	N/A	34.83

[a]R5: $Li_2S_6(sol)_m + nsol \rightarrow S_3^{\bullet-} + Li^+(sol)_p + LiS_3^{\bullet}(sol)_q$.

[b]The lowest ΔG_r are in bold for each NCS in reactants.

Table S13. Reaction free energies (ΔG_r, in kcal/mol) of R6 when considering the solvation structures with all possible NCS.

coefficient in R6[a]				ΔG_r[b]		coefficient in R6				ΔG_r	
m	n	p	q	DMSO	DOL	m	n	p	q	DMSO	DOL
2	0	1	1	**36.00**	**68.64**	5	2	2	5	19.43	47.40
3	0	1	2	**28.67**	**61.22**	5	2	3	4	1.79	39.56
3	0	2	1	**28.67**	**61.22**	5	2	4	3	1.79	39.56
4	0	1	3	23.14	59.01	5	2	5	2	19.43	47.40
4	0	2	2	19.40	58.65	5	2	6	1	36.31	64.66
4	0	3	1	23.14	59.01	5	3	2	6	26.66	58.41
4	1	1	4	18.29	54.79	5	3	3	5	13.51	41.50
4	1	2	3	13.49	52.75	5	3	4	4	**−3.06**	**35.35**
4	1	3	2	13.49	52.75	5	3	5	3	13.51	41.50
4	1	4	1	18.29	54.79	5	3	6	2	26.66	58.41
4	2	1	5	30.01	56.72	5	4	3	6	20.74	52.51
4	2	2	4	8.63	48.54	5	4	4	5	8.66	37.28
4	2	3	3	7.57	46.85	5	4	5	4	8.66	37.28
4	2	4	2	8.63	48.54	5	4	6	3	20.74	52.51
4	2	5	1	30.01	56.72	5	5	4	6	15.89	48.29
4	3	1	6	37.24	67.74	5	5	5	5	20.38	39.21
4	3	2	5	20.35	50.47	5	5	6	4	15.89	48.29
4	3	3	4	2.72	42.64	5	6	5	6	27.61	50.23
4	3	4	3	2.72	42.64	5	6	6	5	27.61	50.23
4	3	5	2	20.35	50.47	5	7	6	6	34.84	61.24
4	3	6	1	37.24	67.74	6	0	1	5	18.91	48.63
4	4	2	6	27.58	61.49	6	0	2	4	−2.46	40.44
4	4	3	5	14.44	44.57	6	0	3	3	−3.53	38.76
4	4	4	4	**−2.13**	**38.42**	6	0	4	2	−2.46	40.44
4	4	5	3	14.44	44.57	6	0	5	1	18.91	48.63
4	4	6	2	27.58	61.49	6	1	1	6	26.14	59.64
4	5	3	6	21.67	55.58	6	1	2	5	9.26	42.38
4	5	4	5	9.59	40.35	6	1	3	4	−8.38	34.54
4	5	5	4	9.59	40.35	6	1	4	3	−8.38	34.54
4	5	6	3	21.67	55.58	6	1	5	2	9.26	42.38
4	6	4	6	16.81	51.37	6	1	6	1	26.14	59.64
4	6	5	5	21.31	42.29	6	2	2	6	16.48	53.39
4	6	6	4	16.81	51.37	6	2	3	5	3.34	36.47
4	7	5	6	28.54	53.30	6	2	4	4	**−13.23**	**30.32**
4	7	6	5	28.54	53.30	6	2	5	3	3.34	36.47
4	8	6	6	35.76	64.32	6	2	6	2	16.48	53.39
5	0	1	4	17.36	51.72	6	3	3	6	10.57	47.49
5	0	2	3	12.56	49.68	6	3	4	5	−1.51	32.26

5	0	3	2	12.56	49.68	6	3	5	4	−1.51	32.26
5	0	4	1	17.36	51.72	6	3	6	3	10.57	47.49
5	1	1	5	29.08	53.65	6	4	4	6	5.72	43.27
5	1	2	4	7.71	45.46	6	4	5	5	10.21	34.19
5	1	3	3	6.64	43.78	6	4	6	4	5.72	43.27
5	1	4	2	7.71	45.46	6	5	5	6	17.44	45.21
5	1	5	1	29.08	53.65	6	5	6	5	17.44	45.21
5	2	1	6	36.31	64.66	6	6	6	6	24.66	56.22

[a]R6: $Li_2S_6(sol)_m + nsol \rightarrow S_3^{\bullet-} + Li^+(sol)_p + S_3^{\bullet-} + Li^+(sol)_q$.

[b]The lowest ΔG_r are in bold for each NCS in reactants.

Table S14. Reaction free energies (ΔG_r, in kcal/mol) of R7 when considering the solvation structures with all possible NCS.

coefficient in R7[a]			ΔG_r[b]	
m	n	p	DMSO	DOL
1	0	1	**10.31**	N/A
2	0	2	**4.89**	N/A
2	1	3	6.20	N/A

[a]R7: $LiS_6^-(DMSO)_m + nDMSO \rightarrow LiS_3^{\bullet}(DMSO)_p + S_3^{\bullet -}$.

[b]The lowest ΔG_r are in bold for each NCS in reactants.

Table S15. Reaction free energies (ΔG_r, in kcal/mol) of R8 when considering the solvation structures with all possible NCS.

coefficient in R8[a]			ΔG_r[b]	
m	n	p	DMSO	DOL
1	0	1	**20.84**	N/A
2	0	2	11.17	N/A
2	1	3	5.26	N/A
2	2	4	**0.41**	N/A
2	3	5	12.13	N/A
2	4	6	19.36	N/A

[a]R8: $LiS_6^-(DMSO)_m + nDMSO \rightarrow S_3^{\bullet-} + Li^+(DMSO)_p + S_3^{\bullet-}$.

[b]The lowest ΔG_r are in bold for each NCS in reactants.

Table S16. Imaginary frequencies (in cm^{-1}) of all transition states.

label	imaginary frequency
TS1[a]	−102.80
TS2[a]	−63.55
TS[b]	−73.51
TS1[c]	−102.61
TS2[c]	−64.50

[a]The transition state refers to the one with the same label in Fig. 4 and S12.
[b]The transition state refers to the one with the same label in Fig. S13 and S16.
[c]The transition state refers to the one with the same label in Fig. S22.

5. Spin-crossing analysis from $^1S_6^{2-*}$ to $^3(S_3^{\bullet-}-S_3^{\bullet-})$ in DMSO

Singlet $^1S_6^{2-*}$ transforms into a triplet complex $^3(S_3^{\bullet-}-S_3^{\bullet-})$ through a spin-state crossing of PESs. Using the single-reference DFT methods (revM06 in this work) is hard to obtain the accurate barrier of this spin-state crossing process. We thus simply estimate the barrier of this process based on the single-state broken symmetry calculations with the spin-contamination correction along the interpolation path from $^1S_6^{2-*}$ to $^3(S_3^{\bullet-}-S_3^{\bullet-})$. In particular, we firstly obtain a series of interpolation structures from $^1S_6^{2-*}$ to $^3(S_3^{\bullet-}-S_3^{\bullet-})$. Then the triplet, singlet, and spin-mixed energies (Fig. S15a) of these interpolation structures are computed. The maximum energy point (denoted as TS2) of the spin-mixed curve exhibits the imaginary vibration toward $^1S_6^{2-*}$ and $^1(S_3^{\bullet-}-S_3^{\bullet-})$. Because of the spin incompleteness, this point is not the pure singlet state. We convert this unphysical spin-mixed energy to pure singlet energy based on the spin-contamination correction.[5,6] After adding the free energy corrections, the spin-crossing process proceeds based on the free energy curve depicted in Fig. S15(b). The estimated barrier (1.99 kcal/mol) is expected to be slightly higher than the actual spin-state crossing barrier because the reaction path is unoptimized.

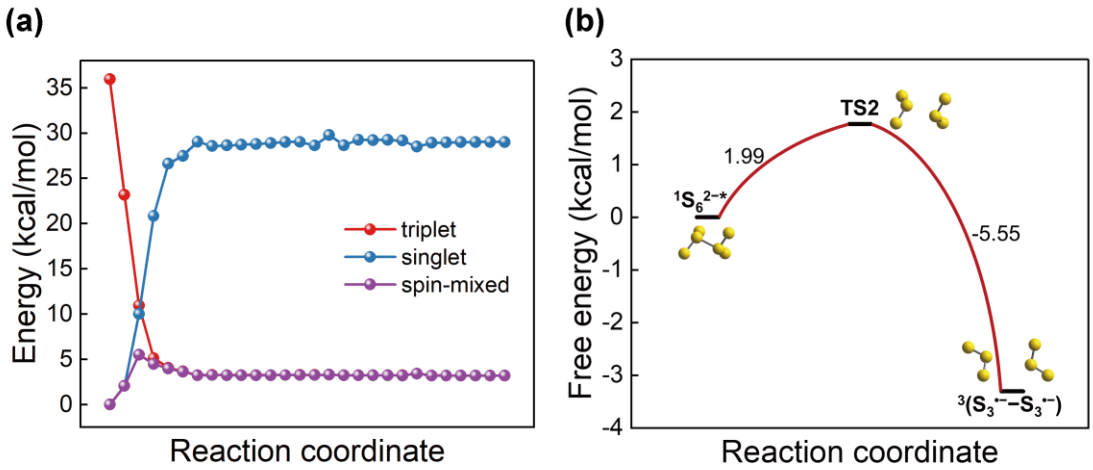

Fig. S15. (a) Potential energies of triplet, singlet, and spin mixed state of S_6^{2-*} with the gradual separation of two $S_3^{\bullet-}$ moieties. (b) Free energy curve of the spin-crossing process. The inset images are optimized structures in DMSO.

6. Generation mechanism of trisulfur radicals in DOL

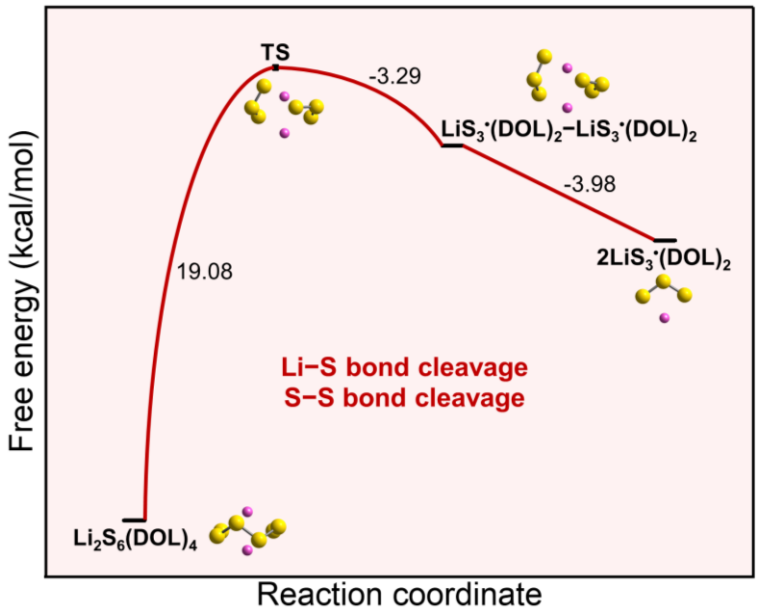

Fig. S16. Proposed generation mechanism of trisulfur radicals in DOL for the reaction of $Li_2S_6(DOL)_4 \rightarrow 2LiS_3^{\bullet}(DOL)_2$. Along the free energy curve, the numbers represent the free energy change of each step. Inset images are optimized structures with explicit DOL molecules not shown for clarity (complete solvation structures are shown in Fig. S13). The whole process involves Li−S bond cleavage and S−S bond cleavage steps.

7. Generation of trisulfur radicals in DMA

To validate the generalizability of the findings in this work, we explore the generation of trisulfur radicals in DMA, another high ε/DN solvent.

We first optimize the solvation structures (see Fig. S17−S21) of all relevant species (Li_2S_6, LiS_6^-, S_6^{2-}, $LiS_3^{\bullet}$, $S_3^{\bullet-}$, and Li^+) in DMA. As shown in Table S17, for Li-containing species, the total binding free energies (G_b) in DMSO and DMA are obviously more negative than those in DOL, while the relative magnitudes of G_b between DMSO and DMA are uncertain, indicating the binding strength between the solvents and sulfur species is largely affected by the DN of solvents but the DN is not the only influencing factor (the DNs of DMSO, DMA, and DOL are 29.8, 27.8 and 18.0 kcal/mol). The solvent structure (such as molecular size, shape) may also influence the binding strength. We also find that all species exhibit very similar solvation behavior in DMA as that in DMSO. Specifically, for Li-containing species, G_b first decreases and then increases with the increasing NCS until the saturation of solvent coordination. For S_6^{2-} and $S_3^{\bullet-}$, their solvation is unfavorable due to the positive G_b. Besides, the results of the best NCS are the same among DMSO, DMA, and DOL, indicating the extremely robust Li-four-coordinated feature in the solvation of Li-containing species.

We further compute the reaction free energies (ΔG_r) of R1−R9 in DMA and the corresponding lowest ΔG_r are shown in Tables S18 and S19. The negative ΔG_r values of R1−R9 mean that Li_2S_6 can spontaneously dissociate into LiS_6^- and S_6^{2-}, and the generation of trisulfur radicals is favorable in DMA. In addition, the dissociation of Li_2S_6 into LiS_6^- and S_6^{2-} as well as the decomposition of hexasulfides to produce trisulfur radicals would be thermodynamically easier when hexasulfides are more fully solvated. These observations are similar to those we find in DMSO, demonstrating the generalizability of our findings.

Fig. S22 displays the detailed reaction mechanism for the reaction $S_6^{2-} \rightarrow 2S_3^{\bullet-}$. The variation trend of free energies along the pathway is again very similar as that in DMSO (see Fig. 4 in the Manuscript). Moreover, the maximum free energy barrier in Fig. S22 is 9.63 kcal/mol, indicating the generation of trisulfur radicals is kinetically feasible in DMA.

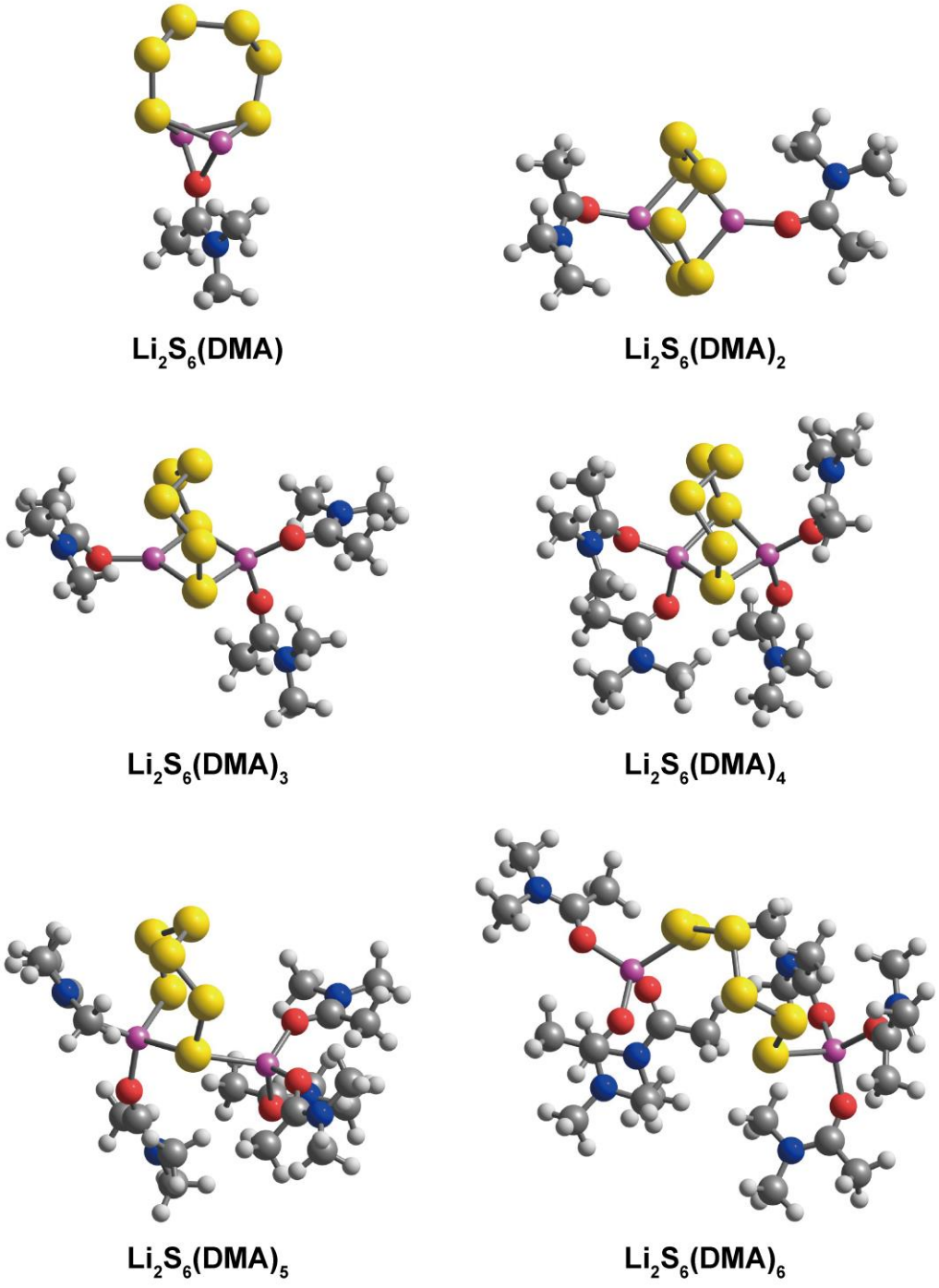

Fig. S17. Optimized solvation structures of Li_2S_6 in DMA.

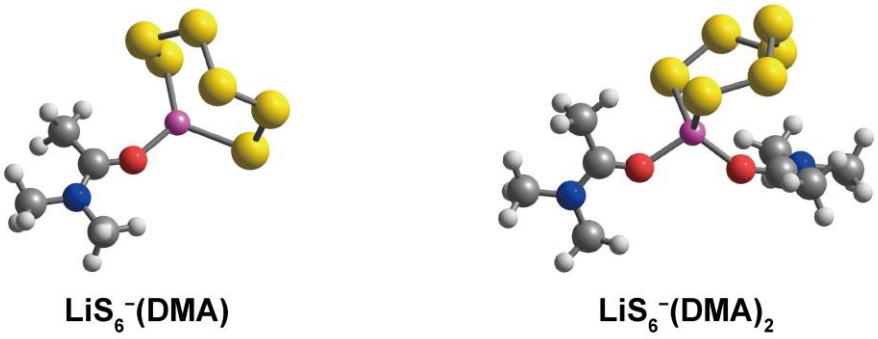

Fig. S18. Optimized solvation structures of LiS_6^- in DMA.

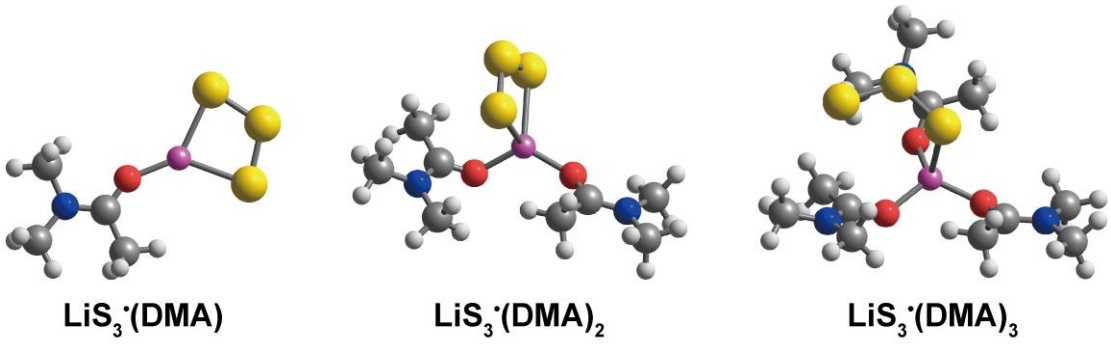

Fig. S19. Optimized solvation structures of $LiS_3^{\bullet}$ in DMA.

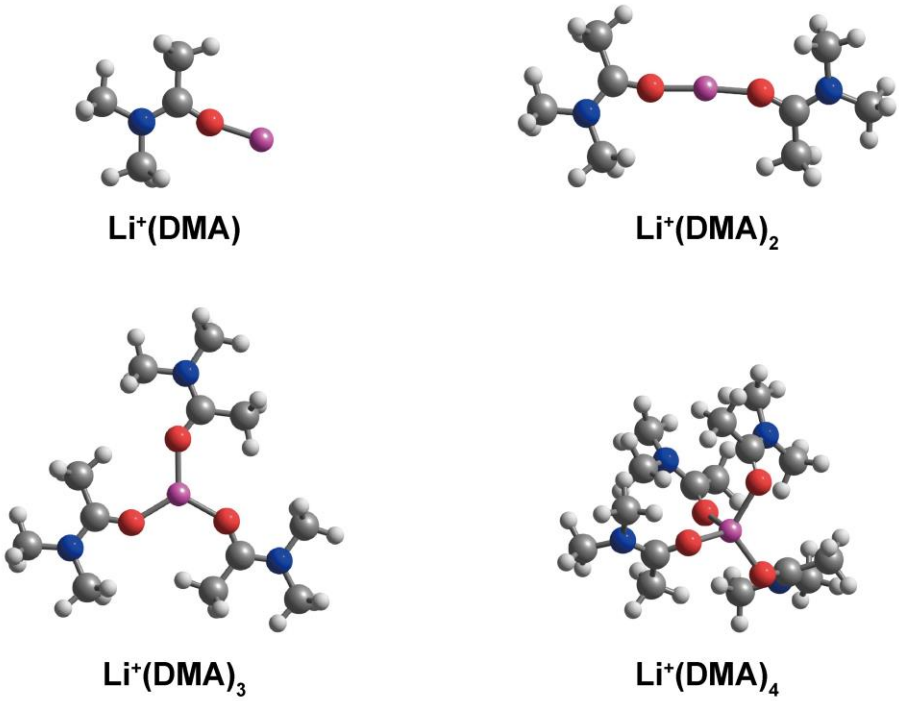

Fig. S20. Optimized solvation structures of Li^+ in DMA.

Fig. S21. Optimized solvation structures of S_6^{2-} and $S_3^{\bullet-}$ in DMA.

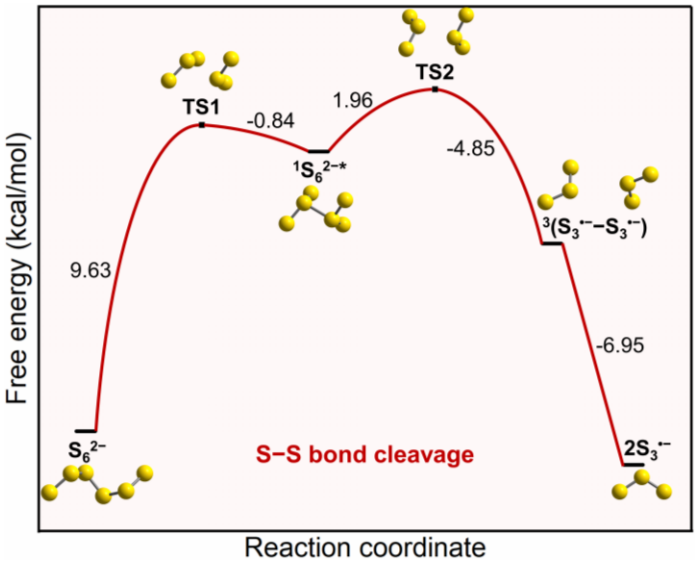

Fig. S22. Proposed generation mechanism of trisulfur radicals in DMA for the reaction of $S_6^{2-} \rightarrow 2S_3^{\bullet-}$. Along the free energy curve, the numbers represent the free energy change of each step. Inset images are optimized structures. The whole pathway is a process of S−S bond cleavage.

Table S17. Total binding free energies [$G_b(n)$, in kcal/mol] and successive binding free energies [$\Delta G_b(n)$, in kcal/mol] with different numbers of coordinated solvents (NCS, n) in DMSO, DMA, and DOL solvents.

solute	n	$G_b(n)$			$\Delta G_b(n)$			best NCS		
		DMSO	DMA	DOL	DMSO	DMA	DOL	DMSO	DMA	DOL
Li_2S_6	1	−5.80	−6.27	−1.76	−5.80	−6.27	−1.76	4	4	4
	2	−18.59	−20.14	−11.86	−12.79	−13.87	−10.11			
	3	−20.91	−20.17	−10.70	−2.32	−0.03	1.16			
	4	−21.29	−22.83	−14.38	−0.38	−2.67	−3.68			
	5	−20.37	−17.96	−11.31	0.93	4.87	3.07			
	6	−10.20	−12.24	−6.29	10.17	5.72	5.02			
LiS_6^-	1	−6.03	−6.22	−2.10	−6.03	−6.22	−2.10	2	2	2
	2	−6.03	−6.35	−3.11	0.00	−0.13	−1.02			
S_6^{2-}	1	5.30	4.98	5.27	5.30	4.98	5.27	N/A	N/A	N/A
$LiS_3^{\bullet}$	1	−9.38	−10.60	−4.85	−9.38	−10.60	−4.85	2	2	2
	2	−14.79	−14.28	−9.64	−5.42	−3.68	−4.79			
	3	−13.48	−14.05	−8.31	1.31	0.23	1.33			
	4	N/A	N/A	−4.77	N/A	N/A	3.54			
$S_3^{\bullet-}$	1	5.15	5.13	4.28	5.15	5.13	4.28	N/A	N/A	N/A
Li^+	1	−14.54	−16.82	−10.02	−14.54	−16.82	−10.02	4	4	4
	2	−24.20	−26.06	−16.27	−9.65	−9.24	−6.25			
	3	−30.11	−31.56	−22.17	−5.92	−5.50	−5.90			
	4	−34.96	−32.37	−26.39	−4.85	−0.81	−4.22			
	5	−23.24	N/A	−24.46	11.72	N/A	1.93			
	6	−16.01	N/A	−13.44	7.23	N/A	11.02			

Table S18. Lowest reaction free energies (ΔG_r, in kcal/mol) of R1−R3 for reactants with different numbers of coordinated solvents (NCS) in DMSO, DMA, and DOL solvents.

label	reaction	ΔG_r		
		DMSO	DMA	DOL
R1	$Li_2S_6(sol)_2 \rightarrow LiS_6^-(sol) + Li^+(sol)$	15.17	14.49	30.42
	$Li_2S_6(sol)_3 \rightarrow LiS_6^-(sol) + Li^+(sol)_2$	7.84	5.28	23.00
	$Li_2S_6(sol)_4 + 2sol \rightarrow LiS_6^-(sol)_2 + Li^+(sol)_4$	−2.54	1.51	15.55
	$Li_2S_6(sol)_5 + sol \rightarrow LiS_6^-(sol)_2 + Li^+(sol)_4$	−3.47	−3.36	12.48
	$Li_2S_6(sol)_6 \rightarrow LiS_6^-(sol)_2 + Li^+(sol)_4$	−13.64	−9.09	7.46
R2	$Li_2S_6(sol)_2 \rightarrow S_6^{2-} + 2Li^+(sol)$	36.49	34.55	76.29
	$Li_2S_6(sol)_3 \rightarrow S_6^{2-} + Li^+(sol) + Li^+(sol)_2$	29.16	25.34	68.87
	$Li_2S_6(sol)_4 + 4sol \rightarrow S_6^{2-} + 2Li^+(sol)_4$	−1.64	6.15	46.07
	$Li_2S_6(sol)_5 + 3sol \rightarrow S_6^{2-} + 2Li^+(sol)_4$	−2.57	1.28	43.00
	$Li_2S_6(sol)_6 + 2sol \rightarrow S_6^{2-} + 2Li^+(sol)_4$	−12.74	−4.45	37.97
R3	$LiS_6^-(sol) \rightarrow S_6^{2-} + Li^+(sol)$	21.33	20.06	45.87
	$LiS_6^-(sol)_2 + 2sol \rightarrow S_6^{2-} + Li^+(sol)_4$	0.90	4.64	30.52

Table S19. Lowest reaction free energies (ΔG_r, in kcal/mol) of R4−R9 for reactants with different numbers of coordinated solvents (NCS) in DMSO, DMA, and DOL solvents.

label	reaction	ΔG_r		
		DMSO	DMA	DOL
R4	$Li_2S_6(sol)_2 \rightarrow 2LiS_3^{\bullet}(sol)$	14.95	12.39	18.85
	$Li_2S_6(sol)_3 \rightarrow LiS_3^{\bullet}(sol) + LiS_3^{\bullet}(sol)_2$	11.86	8.73	12.90
	$Li_2S_6(sol)_4 \rightarrow 2LiS_3^{\bullet}(sol)_2$	6.82	7.71	11.80
	$Li_2S_6(sol)_5 \rightarrow 2LiS_3^{\bullet}(sol)_2 + sol$	5.90	2.84	8.73
	$Li_2S_6(sol)_6 \rightarrow 2LiS_3^{\bullet}(sol)_2 + 2sol$	−4.27	−2.88	3.70
R5	$Li_2S_6(sol)_2 \rightarrow S_3^{\bullet-} + Li^+(sol) + LiS_3^{\bullet}(sol)$	25.48	22.94	43.75
	$Li_2S_6(sol)_3 \rightarrow S_3^{\bullet-} + Li^+(sol)_2 + LiS_3^{\bullet}(sol)$	18.15	13.74	36.33
	$Li_2S_6(sol)_4 + 2sol \rightarrow S_3^{\bullet-} + Li^+(sol)_4 + LiS_3^{\bullet}(sol)_2$	2.35	6.4	25.11
	$Li_2S_6(sol)_5 + sol \rightarrow S_3^{\bullet-} + Li^+(sol)_4 + LiS_3^{\bullet}(sol)_2$	1.42	1.53	22.04
	$Li_2S_6(sol)_6 \rightarrow S_3^{\bullet-} + Li^+(sol)_4 + LiS_3^{\bullet}(sol)_2$	−8.75	−4.19	17.01
R6	$Li_2S_6(sol)_2 \rightarrow 2S_3^{\bullet-} + 2Li^+(sol)$	36.00	33.5	68.64
	$Li_2S_6(sol)_3 \rightarrow 2S_3^{\bullet-} + Li^+(sol) + Li^+(sol)_2$	28.67	24.29	61.22
	$Li_2S_6(sol)_4 + 4sol \rightarrow 2S_3^{\bullet-} + 2Li^+(sol)_4$	−2.13	5.09	38.42
	$Li_2S_6(sol)_5 + 3sol \rightarrow 2S_3^{\bullet-} + 2Li^+(sol)_4$	−3.06	0.22	35.35
	$Li_2S_6(sol)_6 + 2sol \rightarrow 2S_3^{\bullet-} + 2Li^+(sol)_4$	−13.23	−5.5	30.32
R7	$LiS_6^-(sol) \rightarrow LiS_3^{\bullet}(sol) + S_3^{\bullet-}$	10.31	8.45	N/A
	$LiS_6^-(sol)_2 \rightarrow LiS_3^{\bullet}(sol)_2 + S_3^{\bullet-}$	4.89	4.90	N/A
R8	$LiS_6^-(sol) \rightarrow 2S_3^{\bullet-} + Li^+(sol)$	20.84	19.00	N/A
	$LiS_6^-(sol)_2 + 2sol \rightarrow 2S_3^{\bullet-} + Li^+(sol)_4$	0.41	3.59	N/A
R9	$S_6^{2-} \rightarrow 2S_3^{\bullet-}$	−0.49	−1.05	N/A

8. Generation of tetrasulfur and disulfur radicals in DMSO and DOL

In addition to trisulfur radicals, we also explore the generation of tetrasulfur ($LiS_4^{\bullet}$, $S_4^{\bullet-}$) and disulfur ($LiS_2^{\bullet}$, $S_2^{\bullet-}$) radicals from hexasulfides. The relevant reactions are as follows (because we already denoted some reactions in the Manuscript as R1−R9, here we label the following reactions as R10−R17):

$$Li_2S_6 \rightarrow LiS_4^{\bullet} + LiS_2^{\bullet} \quad \text{(R10)}$$

$$Li_2S_6 \rightarrow S_4^{\bullet-} + Li^+ + LiS_2^{\bullet} \quad \text{(R11)}$$

$$Li_2S_6 \rightarrow LiS_4^{\bullet} + S_2^{\bullet-} + Li^+ \quad \text{(R12)}$$

$$Li_2S_6 \rightarrow S_4^{\bullet-} + S_2^{\bullet-} + 2Li^+ \quad \text{(R13)}$$

$$LiS_6^- \rightarrow LiS_4^{\bullet} + S_2^{\bullet-} \quad \text{(R14)}$$

$$LiS_6^- \rightarrow S_4^{\bullet-} + LiS_2^{\bullet} \quad \text{(R15)}$$

$$LiS_6^- \rightarrow S_4^{\bullet-} + S_2^{\bullet-} + Li^+ \quad \text{(R16)}$$

$$S_6^{2-} \rightarrow S_4^{\bullet-} + S_2^{\bullet-} \quad \text{(R17)}$$

The optimized solvation structures of $LiS_4^{\bullet}$, $S_4^{\bullet-}$, $LiS_2^{\bullet}$, and $S_2^{\bullet-}$ with different numbers of coordinated solvents (NCS) are shown in Fig. S23−S28. As shown in Table S20, for $LiS_4^{\bullet}$ and $LiS_2^{\bullet}$, with the increase of NCS, the total binding free energies (G_b) first decreases and then increases until the saturation of solvent coordination. The best NCS of $LiS_4^{\bullet}$ and $LiS_2^{\bullet}$ are two in DMSO and DOL, again indicating that four-coordinated solvation structures of Li are the most stable. As for $S_4^{\bullet-}$ and $S_2^{\bullet-}$, the G_b are positive, indicating that their solvation is energetically unfavorable. These results show that tetrasulfur and disulfur radicals have very similar solvation behavior as trisulfur radicals in DMSO and DOL.

Next, we calculate the reaction free energies (ΔG_r) of R10−R17 based on all possible solvation states of involved species. The corresponding lowest ΔG_r are listed in Table S21. The ΔG_r from hexasulfides to tetrasulfur and disulfur radicals are higher than 4.05 and 16.58 kcal/mol in DMSO and DOL, respectively, demonstrating that the generation of tetrasulfur and disulfur radicals is slightly unfavorable in DMSO and rather unfavorable in DOL. Combining with the results about the trisulfur radical generation (see Table 3 in Manuscript), we conclude that hexasulfides prefer to decompose into trisulfur rather than tetrasulfur and disulfur radicals in DMSO and DOL. This finding may explain why tetrasulfur and disulfur radicals are commonly undetected in Li−S batteries.

Fig. S23. Optimized solvation structures of $LiS_4^{\bullet}$ in DMSO.

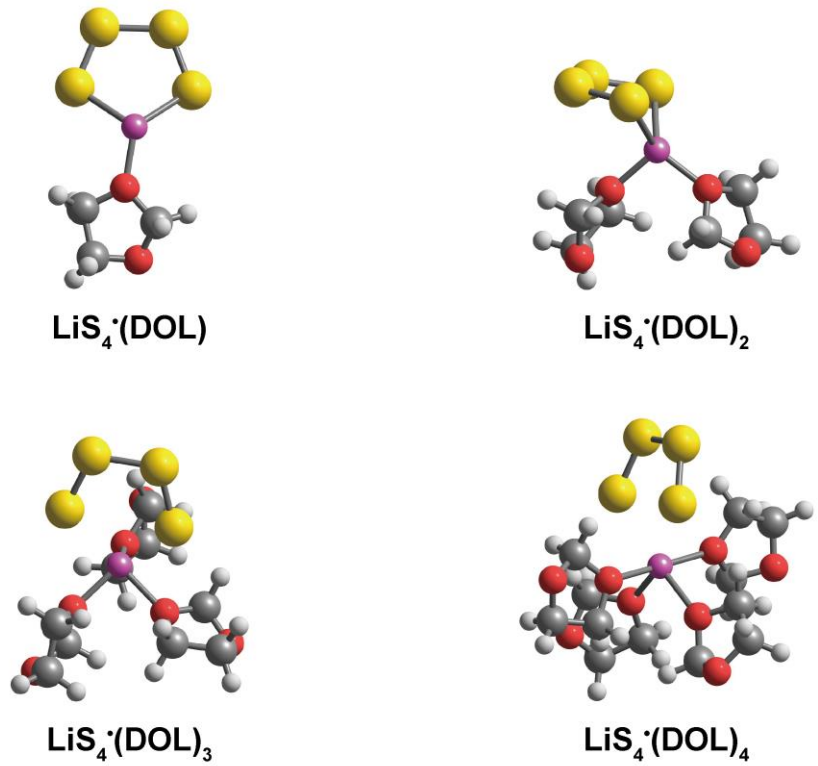

Fig. S24. Optimized solvation structures of $LiS_4^{\bullet}$ in DOL.

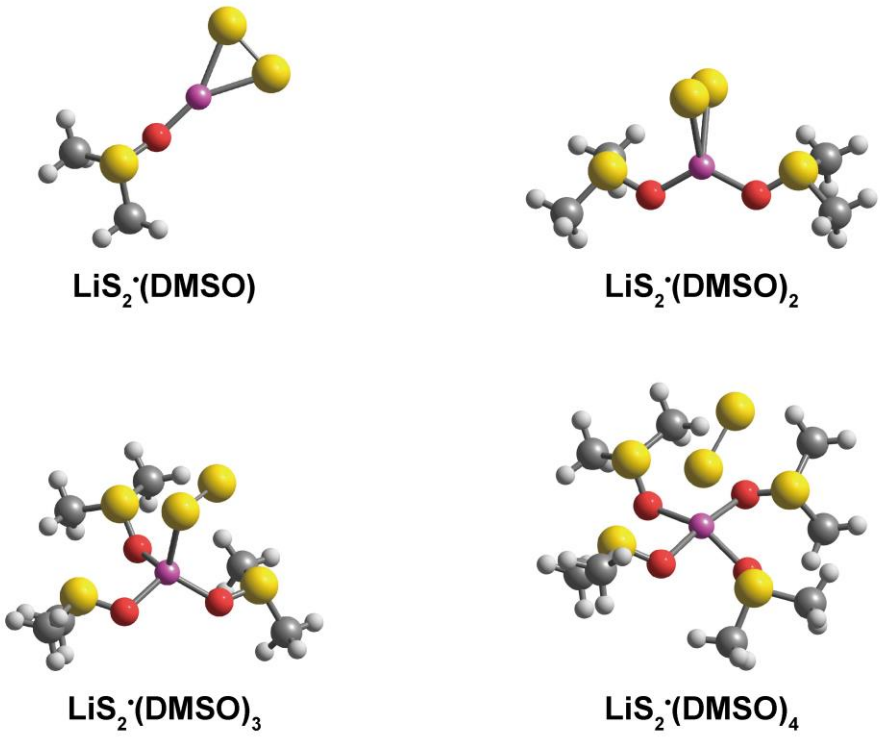

Fig. S25. Optimized solvation structures of $LiS_2^{\bullet}$ in DMSO.

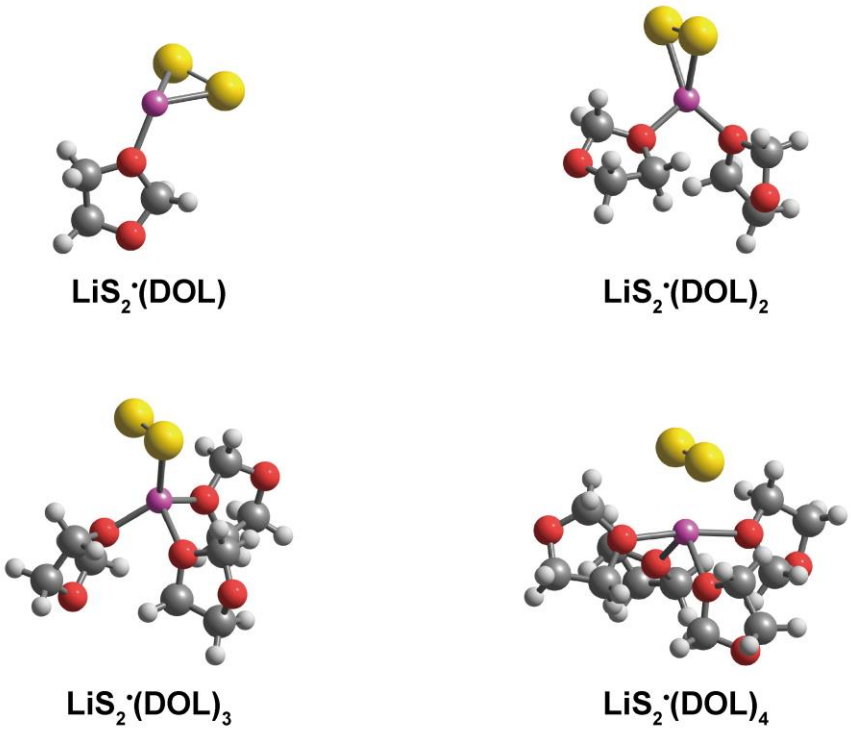

Fig. S26. Optimized solvation structures of $LiS_2^{\bullet}$ in DOL.

Fig. S27. Optimized solvation structures of $S_4^{\bullet-}$ and $S_2^{\bullet-}$ in DMSO.

Fig. S28. Optimized solvation structures of $S_4^{\bullet-}$ and $S_2^{\bullet-}$ in DOL.

Table S20. Total binding free energies [$G_b(n)$, in kcal/mol] and successive binding free energies [$\Delta G_b(n)$, in kcal/mol] with different numbers of coordinated solvents (NCS, n) in DMSO and DOL solvents.

solute	n	$G_b(n)$		$\Delta G_b(n)$		best NCS	
		DMSO	DOL	DMSO	DOL	DMSO	DOL
$LiS_4^{\bullet}$	1	−9.75	−5.21	−9.75	−5.21	2	2
	2	−15.23	−9.74	−5.48	−4.53		
	3	−11.79	−8.45	3.44	1.30		
	4	N/A	−3.69	N/A	4.75		
$S_4^{\bullet-}$	1	5.94	6.29	5.94	6.29	N/A	N/A
$LiS_2^{\bullet}$	1	−10.77	−5.34	−10.77	−5.34	2	2
	2	−14.24	−10.02	−3.47	−4.68		
	3	−12.35	−7.55	1.89	2.47		
	4	−6.24	−4.18	6.11	3.37		
$S_2^{\bullet-}$	1	4.22	4.95	4.22	4.95	N/A	N/A

Table S21. Lowest reaction free energies (ΔG_r, in kcal/mol) of R10−R17 for reactants with different numbers of coordinated solvents (NCS) in DMSO and DOL solvents.

label	reaction	ΔG_r	
		DMSO	DOL
R10	$Li_2S_6(sol)_2 \rightarrow LiS_4^{\bullet}(sol) + LiS_2^{\bullet}(sol)$	25.61	31.36
	$Li_2S_6(sol)_3 \rightarrow LiS_4^{\bullet}(sol)_2 + LiS_2^{\bullet}(sol)$	22.46	25.67
	$Li_2S_6(sol)_4 \rightarrow LiS_4^{\bullet}(sol)_2 + LiS_2^{\bullet}(sol)_2$	19.37	24.68
	$Li_2S_6(sol)_5 \rightarrow LiS_4^{\bullet}(sol)_2 + LiS_2^{\bullet}(sol)_2 + sol$	18.45	21.61
	$Li_2S_6(sol)_6 \rightarrow LiS_4^{\bullet}(sol)_2 + LiS_2^{\bullet}(sol)_2 + 2sol$	8.27	16.58
R11	$Li_2S_6(sol)_2 \rightarrow S_4^{\bullet-} + Li^+(sol) + LiS_2^{\bullet}(sol)$	37.46	56.78
	$Li_2S_6(sol)_3 \rightarrow S_4^{\bullet-} + Li^+(sol)_2 + LiS_2^{\bullet}(sol)$	30.13	49.36
	$Li_2S_6(sol)_4 + 2sol \rightarrow S_4^{\bullet-} + Li^+(sol)_4 + LiS_2^{\bullet}(sol)_2$	16.28	38.25
	$Li_2S_6(sol)_5 + sol \rightarrow S_4^{\bullet-} + Li^+(sol)_4 + LiS_2^{\bullet}(sol)_2$	15.36	35.18
	$Li_2S_6(sol)_6 \rightarrow S_4^{\bullet-} + Li^+(sol)_4 + LiS_2^{\bullet}(sol)_2$	5.18	30.16
R12	$Li_2S_6(sol)_2 \rightarrow LiS_4^{\bullet}(sol) + Li^+(sol) + S_2^{\bullet-}$	41.43	60.48
	$Li_2S_6(sol)_3 \rightarrow LiS_4^{\bullet}(sol) + Li^+(sol)_2 + S_2^{\bullet-}$	34.1	53.06
	$Li_2S_6(sol)_4 + 2sol \rightarrow LiS_4^{\bullet}(sol)_2 + Li^+(sol)_4 + S_2^{\bullet-}$	18.23	42.1
	$Li_2S_6(sol)_5 + sol \rightarrow LiS_4^{\bullet}(sol)_2 + Li^+(sol)_4 + S_2^{\bullet-}$	17.31	39.03
	$Li_2S_6(sol)_6 \rightarrow LiS_4^{\bullet}(sol)_2 + Li^+(sol)_4 + S_2^{\bullet-}$	7.14	34.01
R13	$Li_2S_6(sol)_2 \rightarrow S_4^{\bullet-} + S_2^{\bullet-} + 2Li^+(sol)$	53.28	85.89
	$Li_2S_6(sol)_3 \rightarrow S_4^{\bullet-} + S_2^{\bullet-} + Li^+(sol) + Li^+(sol)_2$	45.95	78.48
	$Li_2S_6(sol)_4 + 4sol \rightarrow S_4^{\bullet-} + S_2^{\bullet-} + 2Li^+(sol)_4$	15.14	55.68
	$Li_2S_6(sol)_5 + 3sol \rightarrow S_4^{\bullet-} + S_2^{\bullet-} + 2Li^+(sol)_4$	14.22	52.6
	$Li_2S_6(sol)_6 + 2sol \rightarrow S_4^{\bullet-} + S_2^{\bullet-} + 2Li^+(sol)_4$	4.05	47.58
R14	$LiS_6^-(sol) \rightarrow LiS_4^{\bullet}(sol) + S_2^{\bullet-}$	26.26	N/A
	$LiS_6^-(sol)_2 \rightarrow LiS_4^{\bullet}(sol)_2 + S_2^{\bullet-}$	20.78	N/A
R15	$LiS_6^-(sol) \rightarrow S_4^{\bullet-} + LiS_2^{\bullet}(sol)$	22.30	N/A
	$LiS_6^-(sol)_2 \rightarrow S_4^{\bullet-} + LiS_2^{\bullet}(sol)_2$	18.82	N/A
R16	$LiS_6^-(sol) \rightarrow S_4^{\bullet-} + S_2^{\bullet-} + Li^+(sol)$	38.11	N/A
	$LiS_6^-(sol)_2 + 2sol \rightarrow S_4^{\bullet-} + S_2^{\bullet-} + Li^+(sol)_4$	17.69	N/A
R17	$S_6^{2-} \rightarrow S_4^{\bullet-} + S_2^{\bullet-}$	16.79	N/A

References

1. Y. Wang, P. Verma, X. Jin, D. G. Truhlar, and X. He, *Proc. Natl. Acad. Sci. U.S.A.*, 2018, **115**, 10257−10262.
2. B. Jeziorski, R. Moszynski, and K. Szalewicz, *Chem. Rev.*, 1994, **94**, 1887−1930.
3. D. G. A. Smith, L. A. Burns, A. C. Simmonett, R. M. Parrish, M. C. Schieber, R. Galvelis, P. Kraus, H. Kruse, R. Di Remigio, A. Alenaizan, A. M. James, S. Lehtola, J. P. Misiewicz, M. Scheurer, R. A. Shaw, J. B. Schriber, Y. Xie, Z. L. Glick, D. A. Sirianni, J. S. O'Brien, J. M. Waldrop, A. Kumar, E. G. Hohenstein, B. P. Pritchard, B. R. Brooks, H. F. Schaefer, A. Y. Sokolov, K. Patkowski, A. E. DePrince, 3rd, U. Bozkaya, R. A. King, F. A. Evangelista, J. M. Turney, T. D. Crawford, and C. D. Sherrill, *J. Chem. Phys.*, 2020, **152**, 184108.
4. A. V. Marenich, S. V. Jerome, C. J. Cramer, and D. G. Truhlar, *J. Chem. Theory Comput.*, 2012, **8**, 527−541.
5. M. Shoji, K. Koizumi, Y. Kitagawa, T. Kawakami, S. Yamanaka, M. Okumura, and K. Yamaguchi, *Chem. Phys. Lett.*, 2006, **432**, 343−347.
6. X. Xu, S. Gozem, M. Olivucci, and D. G. Truhlar, *J. Phys. Chem. Lett.*, 2013, **4**, 253−258.